Brief Communication

Synaptic Activity of the AFD Neuron in *Caenorhabditis elegans* Correlates with Thermotactic Memory

Aravinthan D. T. Samuel, Ruwan A. Silva, and Venkatesh N. Murthy
Department of Molecular and Cellular Biology, Harvard University, Cambridge, Massachusetts 02138

Thermotactic behavior in *Caenorhabditis elegans* is sensitive to both a worm's ambient temperature (T_{amb}) and its memory of the temperature of its cultivation (T_{cult}). The AFD neuron is part of a neural circuit that underlies thermotactic behavior. By monitoring the fluorescence of pH-sensitive green fluorescent protein localized to synaptic vesicles, we measured the rate of the synaptic release of AFD in worms cultivated at temperatures between 15 and 25°C, and subjected to fixed, ambient temperatures in the same range. We found that the rate of AFD synaptic release is high if either $T_{amb} > T_{cult}$ or $T_{amb} < T_{cult}$, but AFD synaptic release is low if $T_{amb} \cong T_{cult}$. This suggests that AFD encodes a direct comparison between T_{amb} and T_{cult}.

Key words: thermotaxis; vesicle recycling; *Caenorhabditis elegans*; GFP; synaptic transmission; exocytosis

Introduction

In a spatial thermal gradient, *Caenorhabditis elegans* moves toward and then tracks isotherms near its temperature of cultivation (T_{cult}). Therefore, the worm is capable of remembering T_{cult} and locating T_{cult} in a thermal gradient. In a current model for thermotaxis, the memory of T_{cult} is encoded as the balance between separate thermophilic and cryophilic drives (Mori, 1999). This model is based on the observation that worms defective in thermotaxis either aggregate at temperatures warmer than T_{cult} (called thermophilic), colder than T_{cult} (called cryophilic), or are insensitive to thermal stimuli (called atactic).

After tracking the movements of worms in response to thermal stimuli, Ryu and Samuel (2002) found that thermotactic behavior comprises two separate mechanisms: (1) for migration down gradients that modulates the frequency but not the direction of turning, and (2) for isothermal tracking that modulates the direction of turning. If the ambient temperature (T_{amb}) > T_{cult}, then the first mechanism is active. If $T_{amb} \cong T_{cult}$, then the second mechanism is active. If $T_{amb} < T_{cult}$, neither mechanism is active. Instead of balancing competing drives, it is possible that worms compare T_{cult} and T_{amb} directly, and activate or inactivate the separate mechanisms underlying thermotaxis on the basis of this comparison.

The AFD neuron has a role in thermotactic behavior. Its absence, attributable either to laser ablation (Mori and Ohshima, 1995) or mutation (Cassata et al., 2000; Satterlee et al., 2001), results in either cryophilic or atactic phenotypes. A calcium-binding protein expressed in several neurons, including AFD, is needed for isothermal tracking (Gomez et al., 2001). Does AFD have a role in thermotactic memory? Does the neuronal activity of AFD encode T_{amb} and/or T_{cult}? Does the pattern of AFD neuronal activity support a model of thermotactic behavior? To answer these questions, we measured the activity of the AFD neuron by measuring the activity of its chemical synapses as a function of temperature.

Chemical synaptic transmission involves synaptic vesicle exocytosis and endocytosis, during which the luminal surface of the vesicle becomes the outer surface of the cell membrane and vice versa. Because the synaptic vesicle lumen is more acidic than the extracellular environment, a particle attached to the luminal surface of a synaptic vesicle undergoes an alkaline pH shift on exocytosis. By attaching a pH-sensitive green fluorescent protein (GFP) to the luminal surface, Miesenbock et al. (1998) could visualize vesicle exocytosis and endocytosis as fluorescence changes at the synapse. Specific attachment to the luminal surface is accomplished by protein fusion to the C terminal of vesicle-associated membrane protein (VAMP).

One version of pH-sensitive GFP, "superecliptic pHluorin," is both more fluorescent and more easily photobleached at the cell surface than inside vesicles (acidity inhibits photon absorption) (Sankaranarayanan et al., 2000). Briefly exposing a synapse containing this VAMP::pHluorin to intense excitation light lowers its fluorescence, but by photobleaching pHluorin at the surface membrane more rapidly than pHluorin inside vesicles. With exocytosis, the fluorescence at the synapse recovers as unbleached pHluorin moves to the surface membrane. The rate of fluorescence recovery after photobleaching (FRAP) thus indicates the rate of exocytosis and the rate of chemical synaptic release. Here, we have used this technique in *C. elegans* and verified it with hippocampal cultured neurons. This technique might also be useful for measuring the rate of synaptic release in other systems.

Received July 16, 2002; revised Oct. 31, 2002; accepted Nov. 1, 2002.

This work was supported by a Mind, Brain, and Behavior Undergraduate Research Fellowship (R.A.S.), by an Amgen Fellowship from the Life Sciences Research Foundation (A.D.T.S.), and by the National Institutes of Health, the Sloan Foundation, and the Pew Scholars program (V.N.M.). We thank Will Ryu and the Rowland Institute Machine Shop for designing and constructing the temperature-controlled stage, Stu Milstein for supervising the mating crosses with unc-13, Juan Burrone for helping with data analysis, Craig Hunter (Harvard University) and Theresa Stiernagle (*Caenorhabditis* Genetics Center) for providing strains, Yishi Jin for providing the VAMP::GFP plasmid, and Brian Chen for commenting on this manuscript.

Correspondence should be addressed to Venkatesh N. Murthy, Harvard University, 16 Divinity Avenue, Cambridge, MA 02138. E-mail: vnmurthy@fas.harvard.edu.

Copyright © 2003 Society for Neuroscience 0270-6474/03/230373-04$15.00/0

Materials and Methods

Molecular biology. We made two plasmids to express VAMP::pHluorin specifically in the synaptic vesicles of the AFD neuron by modifying a construct encoding VAMP::enhanced GFP (EGFP) under the control of the *unc-25* promoter (obtained from Yishi Jin, University of California, Santa Cruz, CA). First, we excised the EGFP sequence and substituted the coding sequence for superecliptic pHluorin (obtained from James Rothman, Sloan-Kettering Institute, New York, NY). Second, we excised the *unc-25* promoter sequence and substituted 1.7 kb of the promoter region for *nhr-38* (resulting in the plasmid pRS1) and 3.7 kb of the promoter region for *gcy-8* (resulting in the plasmid pRS2). Both promoters drive expression specifically in the AFD neuron (Yu et al., 1997; Miyabayashi et al., 1999).

Strains, cultivation, and experimental preparation. We transformed N2 worms using conventional DNA injection methods with pRS1, pRS2, and a plasmid containing the rol-6 marker at concentrations of ~20, ~20, and 100 ng/μl, respectively (Mello and Fire, 1995). DNA transformation with pRS1 and pRS2 led to fluorescent labeling of AFD synapses consistent with the localization of VAMP::pHluorin to synaptic vesicles (Nonet, 1999). In all experiments, we used the progeny of a single transmitting line. For the control experiment, we introduced the *unc-13(e450)* mutation by crossing the transmitting line with the strain CB450. N2 worms were obtained from Craig Hunter (Harvard University, Cambridge, MA). Strain CB450 was obtained from Theresa Stiernagle at the *Caenorhabditis* Genetics Center (University of Minnesota, St. Paul, MN).

The strains were grown and maintained as described by Sulston and Hodgkin (1988). The day before an experiment, worms were moved to a normal growth medium (NGM) cultivation plate covered with ample food (a bacterial lawn of OP50), materials described by Sulston and Hodgkin (1988). These plates were incubated overnight at 15, 20, or 25°C to set T_{cult}. In each experiment, a young adult was selected from the cultivation plate, rinsed in NGM buffer (containing the same inorganic ion concentration as the NGM cultivation plates), and embedded in a gel containing NGM buffer, 1% low melting point agarose, and 0.01% levamisole. Embedding occurred near the gelling temperature of the agarose (<30°C) to avoid damaging the worm. In experiments with starved worms, the protocol was the same except that the worms were moved to bare NGM plates 4 hr before an experiment.

The microscope slide containing the embedded worm was placed on a temperature-controlled stage. The stage comprised a 3 × 0.5 inch hollow brass block. Water of fixed temperatures was pumped through the hollow of the block with a circulating water bath. Thus, the temperature of the embedded worm could be fixed to temperatures of 1, 2, or 25°C with stability of <0.1°C; these conditions were verified with measurements using a T-type thermocouple.

The time between selecting the worm from the cultivation plate to embedding the worm was <10 min. Imaging continued for approximately another 10 min.

Microscopy and data analysis. The embedded worm was imaged using a confocal microscope (Fluoview; Olympus America, Melville, NY) attached to a BX50-WI upright microscope, using a 40×, 0.8 numerical aperture (NA) water immersion lens. The 488 nm line of an argon laser was used for excitation and photobleaching. Emission was filtered with a 505–550 nm bandpass filter.

First, the synapses of AFD were imaged, recognizable as bright fluorescent puncta along the neuronal process expected to contain presynaptic terminals (Fig. 1). We did not distinguish the left AFD neuron from the right AFD neuron, choosing whichever neuron was at the shallower imaging depth. Next, a synapse was selected for experimentation based on its clarity and distinctness from neighboring synapses. Most or all of these synapses likely contacted the AIY neuron that also has a role in thermotactic signaling (Mori and Ohshima, 1995): of the 20 presynaptic terminals of AFD, 17 contact AIY (White et al., 1986). The selected synapse was photobleached by raising laser intensity ~10-fold and until its fluorescence dropped by ~50%. Finally, the synapse was imaged at intervals after photobleaching by capturing an image stack (a cube 10 μm on edge) centered on it; this would ensure that the selected synapse did not leave the imaging volume during the experiment.

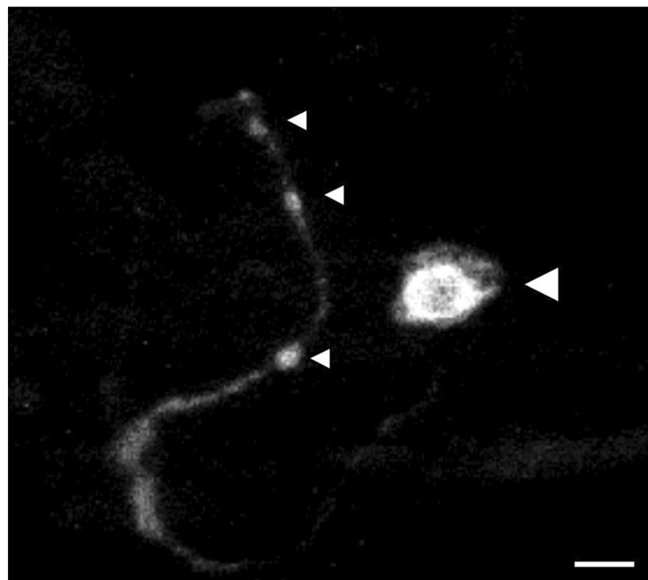

Figure 1. Confocal image of an AFD neuron expressing VAMP::pHluorin before photobleaching. This maximal projection of 20 (1 μm) sections contains the cell body (*large arrowhead*), neuronal process, and synapses along the process (*small arrowheads*). Scale bar, 2 μm. The brightness of the image is attributable to high gain (~700 V applied to the photomultiplier tubes) and not to excessive expression of the VAMP::pHluorin.

Afterward, using the Fluoview analysis package, we quantified the fluorescence of the selected synapse by measuring the average intensity of a region of interest containing it (1 × 1 μm square in the *z*-section containing the synapse). We calculated FRAP in fractional units using the following equation: $[f(t) - f_p]/[f_i - f_p]$, where f_i is the fluorescence at the synapse before photobleaching, f_p is the fluorescence at the synapse immediately after photobleaching, and $f(t)$ is the fluorescence at the synapse at time t after photobleaching. Statistics were calculated with MatLab (MathWorks Inc., Natick, MA).

Hippocampal neuron culture and transfection. Hippocampal neurons were dissociated from 1- to 3-d-old rats using methods described previously (Li and Murthy, 2001). Neurons were transfected at 6–7 d *in vitro* using the calcium phosphate method (Xia et al., 1996). Transfected cultures were allowed to grow for another week, allowing mature synapses to develop. Experiments were performed when cells were 13–15 d *in vitro*, and at room temperature (20–22°C).

Hippocampal neuron imaging. For the imaging experiments, coverslips with neurons were mounted in a custom-built chamber, and a pair of platinum wires separated by ~5 mm was placed above the coverslip for extracellular stimulation. All experiments were done in HEPES-buffered saline containing (in mM): 136 NaCl, 2.5 KCl, 10 HEPES, 10 D-glucose, 2 $CaCl_2$, and 1.3 $MgCl_2$, and also containing 50 μM APV and 10 μM CNQX to block recurrent activity. A Grass SD9 stimulator (Grass Instruments, West Warwick, RI) was used to evoke action potentials, using brief voltage pulses (1 msec, 20–50 V, bipolar) applied to the platinum wires.

Images were acquired using a confocal microscope (Fluoview; Olympus) attached to a BX50-WI upright microscope, using a 40×, 0.8 NA water immersion lens. The 488 nm line of an argon laser was used for excitation, and the emitted light was filtered with a 505–550 bandpass filter. After identifying synaptic boutons expressing VAMP::pHluorin, selected boutons were photobleached by raising the laser intensity by ~10-fold. Subsequently, either no stimulus was presented, or we evoked action potentials in the neurons at 4 or 10 Hz. Images were analyzed in the same manner as for AFD synapses (see above).

Results

We localized VAMP::pHluorin to synapses of AFD by expressing it under the control of AFD-specific promoters. We were then able to monitor chemical synaptic release of the AFD neuron by

J. Neurosci., January 15, 2003 • 23(2):373–376 • **375**

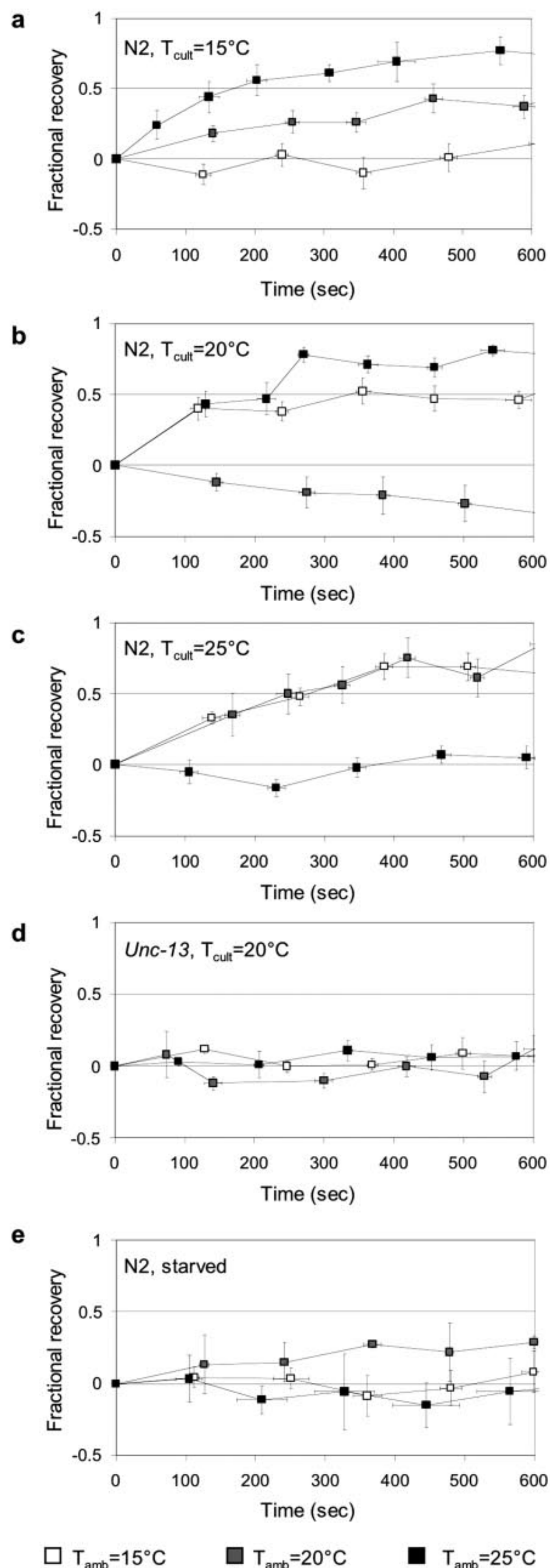

Figure 2. FRAP of synapses of the AFD neuron containing VAMP::pHluorin and subjected to fixed ambient temperatures of 15°C (*white squares*), 20°C (*gray squares*), and 25°C (*black squares*). The *panels* separate experiments as follows: *a*, N2 worms cultivated overnight at 15°C; *b*, N2 worms cultivated overnight at 20°C; *c*, N2 worms cultivated overnight at 25°C; *d*, *unc-13* worms cultivated overnight at 20°C; *e*, N2 worms starved for 4 hr at 20°C. In *a*–*d*, 18 worms were studied, six at each value of T_{amb}. In *e*, nine worms were studied, three at each value of T_{amb}. In each *panel*, the *abscissa* is the time course of the experiment, where $t = 0$ sec corresponds to the photobleaching. The *ordinate* is the fractional recovery of FRAP calculated for each time point, as described in Materials and Methods. Error bars indicate SEM. In *a*–*c*, significant recovery was measured in the cases $T_{amb} \neq T_{cult}$, but negligible recovery was measured when $T_{amb} = T_{cult}$. In *d* and *e*, negligible recovery was measured regardless of T_{amb}. In cases of fluorescence recovery, exponential fits gave coarse estimates of the rates of recovery (Table 1).

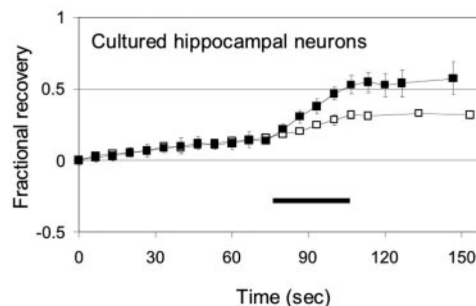

Figure 3. Fluorescence recovery after photobleaching of synapses of cultured hippocampal neurons expressing VAMP::pHluorin. The *bar* indicates an interval during which action potentials were evoked at 4 Hz (□) or 10 Hz (■). The *abscissa* is the time course of the experiment, where $t = 0$ sec corresponds to the photobleaching. The *ordinate* is the FRAP. Error bars indicate the SEM of 10 synapses from two experiments at each rate of stimulation. Stimulation increases the rate of recovery beyond the spontaneous rate. The amount of recovery after 30 sec of 10 Hz stimulation exceeds the amount of recovery after 30 sec of 4 Hz stimulation, suggesting that more vesicles fused to the membrane with the higher-frequency stimulation. This supports the use of the rate of recovery as a measure of the amount of synaptic release in a neuron.

measuring the amount of FRAP of VAMP::pHluorin at AFD synapses in several experimental conditions.

We verified that FRAP correlates with synaptic release. First, we measured FRAP in a strong *unc-13* mutant background. Unc-13 is required for exocytosis (Richmond et al., 1999). The *unc-13* mutation does not noticeably disrupt the number, position, or distinctness of fluorescent puncta corresponding to synapses, suggesting that the *unc-13* does not disrupt synapse formation in AFD. As expected, FRAP is abolished in an *unc-13* background (Fig. 2*d*). Second, FRAP is abolished in worms anesthetized with sodium azide (data not shown). Third, verifying the method with hippocampal cultured neurons, we found that FRAP follows synaptic release evoked by action potential stimuli (Fig. 3).

Does FRAP, and thus the chemical synaptic release of the AFD neuron, depend on either a worm's ambient temperature (T_{amb}) or the worm's memory of its cultivation temperature (T_{cult})? We cultivated worms overnight at 15, 20, or 25°C to set T_{cult} and during experiments set T_{amb} to 15, 20, or 25°C with a temperature-controlled stage. For worms cultivated at 15°C, the FRAP was least at 15°C, and higher at 20 or 25°C (Fig. 2*a*). For worms cultivated at 20°C, the FRAP was least at 20°C, and higher at 15 or 25°C (Fig. 2*b*). For worms cultivated at 25°C, the FRAP was least at 25°C, and higher at 15 or 20°C. The pattern of AFD activity depends on both T_{amb} and T_{cult}: AFD is more active when $T_{amb} > T_{cult}$ or $T_{amb} < T_{cult}$ and less active when $T_{amb} \cong T_{cult}$.

Worms starved for ≥4 hr forget T_{cult} (Hedgecock and Russell, 1975). We studied worms starved for 4 hr at 20°C and tested at T_{amb} of 15, 20, or 25°C. In starved worms, FRAP was negligible in the AFD neuron regardless of T_{amb} (Fig. 2*e*).

Table 1 summarizes all experimental data from Figure 2.

Table 1. Summary of Figure 2, tabulating both the magnitudes and rates of fluorescence recovery

	T_{amb}		
	15°C	20°C	25°C
N2 T_{cult}			
15°C	0	$+$ $\tau = 594$	$++$ $\tau = 437$
20°C	$+$ $\tau = 1028$	0	$++$ $\tau = 368$
25°C	$++$ $\tau = 355$	$++$ $\tau = 155$	0
N2, starved	0	0	0
Unc-13	0	0	0

The symbols $++$, $+$, and 0 correspond to $>$50% recovery, 10–50% recovery, and $<$10% recovery, respectively, at ~400 sec after photobleaching. The time 400 sec was chosen arbitrarily. In cases of fluorescence recovery, $+$ or $++$, the time constant of recovery was estimated with exponential fits using the form $1 - \exp(-t/\tau)$. The resulting values of τ (in seconds) provide a coarse estimate of the duration of a round of synaptic vesicle recycling.

Discussion

In worms with a memory of T_{cult}, our results indicate that AFD carries at least one bit of information: AFD is "on" when the $T_{amb} \neq T_{cult}$ and "off" when $T_{amb} = T_{cult}$. Starvation disrupts the memory of T_{cult}, and we found that it also disrupts the pattern of AFD activity. In starved worms, AFD is always off, regardless of T_{amb}. This pattern of AFD activity, because it is dependent on both thermal stimulus and thermal experience, might be relevant to the thermotactic program, because AFD is known to have a role in this program.

Because its laser ablation or absence attributable to mutation generates cryophilic phenotypes (Mori and Ohshima, 1995), AFD has been regarded as a thermophilic component in the model of competing thermophilic and cryophilic drives. That is, when AFD signaling is turned off, the absence of thermophilic signaling leads to the domination of the cryophilic drive on the worm's movements. However, this study suggests that AFD signaling is on in the temperature regimen $T_{amb} > T_{cult}$ when the cryophilic drive should dominate the worm's movements. One possibility is that the cryophilic drive exceeds the thermophilic drive in signal intensity in this regimen.

Ryu and Samuel (2002) found that thermotaxis comprises two separate mechanisms, and that the pattern of activity of these mechanisms depends on both T_{amb} and T_{cult}. In their view, the mechanism for isothermal tracking is active when $T_{amb} = T_{cult}$, the mechanism for migration down gradients is active when $T_{amb} > T_{cult}$, and neither is active when $T_{cult} < T_{amb}$. One might speculate that the on–off pattern of AFD activity is part of a Boolean computation that determines the on–off states of underlying behavioral mechanisms.

Thermotaxis requires more information than we have resolved resides in the AFD neuron. The worm distinguishes $T_{amb} > T_{cult}$ from $T_{amb} < T_{cult}$, and whether T_{amb} is rising or falling (Ryu and Samuel, 2002). AFD might encode some of this information in ways that we could not resolve. For instance, AFD signaling might be different when T_{amb} is above or below T_{cult} if signaling is sensitive to the timing and not only the rate of synaptic release. AFD might also be sensitive to temporal thermal gradients, but in this study we fixed T_{amb}.

The worm is capable of remembering T_{cult}, measuring T_{amb}, and comparing T_{amb} with T_{cult}. We do not know whether these functions are performed by AFD or neurons presynaptic to AFD (e.g., AIN, AWA, or AIB) (White et al., 1986). It is likely that the neural circuit underlying thermotaxis encodes T_{cult} by associating temperature with a condition of cultivation (e.g., sensations corresponding to ingestion, digestion, or metabolism of food). If so, the thermal circuit might require inputs from neurons that signal the associated condition. Alternatively, AFD might perform the association without synaptic input, perhaps using an internal metabolic cue.

It is difficult to speculate about the significance of the pattern of AFD activity without similar information from other neurons. Is the pattern unique to AFD, or is it shared by other neurons? How does the activity of other thermotaxis neurons compare with AFD? On the basis of these comparisons, how does the worm make thermotactic decisions? Techniques for measuring neuronal activity in worms are being developed and will eventually answer these questions (Kerr et al., 2000).

References

Cassata G, Kagoshima H, Andachi Y, Kohara Y, Durrenberger MB, Hall DH, Burglin TR (2000) The LIM homeobox gene ceh-14 confers thermosensory function to the AFD neurons in *Caenorhabditis elegans*. Neuron 25:587–597.

Gomez M, DeCastro E, Guarin E, Sasakura H, Kujara A, Mori I, Bartfai T, Bargmann CI, Nef P (2001) Ca^{2+} signaling via the neuronal calcium sensor ncs-1 regulates associative learning and memory in *C. elegans*. Neuron 30:241–248.

Hedgecock EM, Russell RL (1975) Normal and mutant thermotaxis in the nematode *Caenorhabditis elegans*. Proc Natl Acad Sci USA 72:4061–4065.

Kerr R, Lev-Ram V, Baird G, Vincent P, Tsien RY, Schafer WR (2000) Optical imaging of calcium transients in neurons and pharyngeal muscle of *C. elegans*. Neuron 26:583–594.

Li Z, Murthy VN (2001) Visualizing postendocytic traffic of synaptic vesicles at hippocampal synapses. Neuron 31:593–605.

Mello CC, Fire A (1995) DNA transformation. In: *Caenorhabditis elegans*: modern biological analysis of an organism (Epstein HF, Shakes DC, eds), pp 452–482. New York: Academic.

Miesenbock G, DeAngelis DA, Rothman JE (1998) Visualizing secretion and synaptic transmission with pH-sensitive green fluorescent proteins. Nature 394:192–195.

Miyabayashi T, Palfreyman MT, Sluder AE, Slack F, Sengupta P (1999) Expression and function of members of a divergent nuclear receptor family in *Caenorhabditis elegans*. Dev Biol 215:314–331.

Mori I (1999) Genetics of chemotaxis and thermotaxis in the nematode *Caenorhabditis elegans*. Annu Rev Genet 33:399–422.

Mori I, Ohshima Y (1995) Neural regulation of thermotaxis in *Caenorhabditis elegans*. Nature 376:344–348.

Nonet ML (1999) Visualization of synaptic specializations in live *C. elegans* with synaptic vesicle protein-GFP fusions. J Neurosci Methods 89:33–40.

Richmond JE, Davis WS, Jorgensen EM (1999) UNC-13 is required for synaptic vesicle fusion in *C. elegans*. Nat Neurosci 2:959–964.

Ryu WS, Samuel ADT (2002) Thermotaxis in *Caenorhabditis elegans* analyzed by measuring responses to defined thermal stimuli. J Neurosci 22:5727–5733.

Sankaranarayanan S, De Angelis D, Rothman JE, Ryan TA (2000) The use of pHluorins for optical measurements of presynaptic activity. Biophys J 79:2199–2208.

Satterlee JS, Sasakura H, Kuhara A, Berkeley M, Mori I, Sengupta P (2001) Specification of thermosensory neuron fate in *C. elegans* requires ttx-1, a homolog of otd/Otx. Neuron 31:943–956.

Sulston J, Hodgkin J (1988) Methods. In: The nematode *Caenorhabditis elegans* (Wood WB, ed), pp 587–606. Cold Spring Harbor, NY: Cold Spring Harbor Laboratory.

White JG, Southgate E, Thomson JN, Brenner S (1986) The structure of the nervous system of the nematode *Caenorhabditis elegans*. Phil Trans R Soc Lond B Biol Sci 314:1–340.

Xia Z, Dudek H, Miranti CK, Greenberg ME (1996) Calcium influx via the NMDA receptor induces immediate early gene transcription by a MAP kinase/ERK-dependent mechanism. J Neurosci 16:5425–5436.

Yu S, Avery L, Baude EJ, Garbers DL (1997) Guanylyl cyclase expression in specific sensory neurons: a new family of chemosensory receptors. Proc Natl Acad Sci USA 94:3384–3387.